Journal of Sound and Vibration 331 (2012) 1759–1776

Contents lists available at SciVerse ScienceDirect

Journal of Sound and Vibration

journal homepage: www.elsevier.com/locate/jsvi

Design of composite laminates for optimum frequency response

Rengin Kayikci, Fazil O. Sonmez *

Department of Mechanical Engineering, Bogazici University, Istanbul, Bebek 34342, Turkiye

ARTICLE INFO

Article history:
Received 30 August 2009
Received in revised form
15 September 2011
Accepted 14 December 2011
Handling Editor: I. Trendafilova
Available online 12 January 2012

ABSTRACT

In this study, natural frequency response of symmetrically laminated composite plates was optimized. An analytical model accounting for bending–twisting effects was used to determine the laminate natural frequency. Two different problems, fundamental frequency maximization and frequency separation maximization, were considered. Fiber orientation angles were chosen as design variables. Because of the existence of numerous local optimums, a global search algorithm, a variant of simulated annealing, was utilized to find the optimal designs. Results were obtained for different plate aspect ratios. Effects of the number of design variables and the range of values they may take on the optimal frequency were investigated. Problems in which fiber angles showed uncertainty were considered. Optimal frequency response of laminates subjected to static loads was also investigated.

1. Introduction

In structures like aircrafts and spacecrafts where thin plates are used, vibration problems become more important. Fundamental frequency gets lower with decreased thickness. Considering that continuous fiber reinforced plates are usually desired for applications requiring high specific strength and stiffness and for this reason they should be designed as thin as possible, they are liable to fail due to resonance under external excitation. Choosing a large thickness far beyond the requirements of strength is against the requirements of light weight and cost effective design. By optimally designing the material system such as material type and its composition, fiber orientations, and stacking sequence, one can optimize the frequency response to avoid resonance without any need to increase the thickness.

If the forcing frequency is not high, by maximizing the natural frequency, the likelihood of resonance can be decreased. Accordingly, some of the researchers [1–20] focused on maximizing the fundamental frequency of laminates. Bert [1] presented results for the maximum fundamental frequency of a simply supported symmetric balanced laminate with a lay-up configuration of $[\pm\theta]_s$. Bert [2] considered the same problem for clamped plates. In both of these studies, bending–twisting effects were approximated with the help of previously known frequencies to obtain a closed-form solution, so a-priori knowledge about the fundamental frequency of laminates having certain stacking sequences was needed. Reiss and Ramachandran [3] obtained the optimum design using a closed-form solution for the laminate frequency. Mateus et al. [4] studied the optimal design of thin laminated plates and obtained results for maximum fundamental frequency and minimum elastic strain energy using finite element method to determine the frequency response. Soares et al. [5] presented a two-level approach for maximizing the natural frequency and minimizing the volume of a plate or shell structure. These studies [3–5] considered the same laminate configuration as the one considered by Bert [1]. Rao and Singh [6]

* Corresponding author. Tel.: +90 212 359 7196; fax: +90 212 287 2456.
E-mail address: sonmezfa@boun.edu.tr (F.O. Sonmez).

0022-460X/$ - see front matter
doi:10.1016/j.jsv.2011.12.020

minimized the weight of a plate subject to a constraint on fundamental frequency by taking the lamina thicknesses as design variables.

If the frequency of the external excitation is high, the structure may be designed so that the external frequency is between two adjacent higher order natural frequencies. In that case, maximizing the interval between these frequencies reduces the risk of resonance. Accordingly, some researchers [18–23] considered the problem of maximum frequency separation. Adali and Verijenko [21] determined the optimum stacking sequences for maximum fundamental frequency and maximum frequency separation of symmetric hybrid laminates undergoing free vibrations. They restricted the fiber orientations to preselected four different angles to save from computational time.

Because analysis and optimization methods for buckling problems can be adapted to vibration problems, a number of studies on buckling of composites [24–26] are also reviewed. In many of the previous studies, in order to find the optimum design, gradient-based search techniques [4,5,7,24] or enumeration (trial of all configurations) [21] were used as optimization methods. Layerwise optimization method [8–10,22,25] was also applied. In this method, the optimum angles were found from outer layer to inner layer with one-dimensional search in order to save computational time. Use of enumeration method ensures finding the best design, but takes a very long time and becomes infeasible for large design spaces. Deterministic algorithms are sensitive to the starting point; for this reason, they most probably converge to a worse local minimum near the starting point rather than the global optimum in a complex design space.

Because the search algorithms were usually suitable only for continuous optimization variables, design optimization of composite laminates was many times formulated as a continuous optimization problem [1–7,11,14,23,24] by taking ply thicknesses and orientation angles as continuous variables. Since a laminate is a stack of plies with a given thickness, ply thicknesses of the final designs had to be rounded to the nearest discrete value. Fiber orientations had also to be chosen within a finite set of angles due to manufacturing constraints. After rounding off the optimized values of continuous design variables, the resulting design may not be an optimum design and the constraints may even be violated. For these reasons, in many studies, optimization of composites was formulated as a discrete optimization problem [8–10,16,17,21,22,25–32].

Stochastic search algorithms are better alternatives to traditional search techniques because they can find the globally optimal configuration without being sensitive to the starting point; they are suitable for discrete optimization problems, and they do not need derivatives of the objective function. They have been used successfully in optimization problems having complex design spaces. However, their computational costs are very high in comparison to deterministic algorithms. Researchers used various stochastic algorithms, genetic algorithms (GA) [16,26–28], simulated annealing (SA) [29–31], and particle swarm optimization [32] in composite optimization. Simulated annealing is inspired from the physical annealing process. In each iteration, a random configuration is generated in the neighborhood of the current configuration. The probability of acceptance of a new configuration is based on the probability of Boltzmann distribution. If the temperature parameter is decreased slowly enough, the Boltzmann distribution tends to converge to a uniform distribution on the set of globally minimal states [33]. Although such a cooling schedule is inefficient, it enables to control the quality of designs with a temperature parameter. Because there is no such control parameter in GA, premature convergence to a local optimum is likely [34]. The distinct advantage of GA over SA is that GA maintains a population of candidate solutions during iterations while simulated annealing keeps only one [34]. As a result, in SA, many good configurations are lost when they are replaced by worse configurations especially at the early stages of optimization. Because both of the algorithms have their own advantages and disadvantages, some researchers tried to combine their advantageous aspects and presented hybrid algorithms that exhibited the characteristics of both of them [33–35]. In the present study, in order to avoid the disadvantage of maintaining a single current configuration in the ordinary simulated annealing algorithm, a set of current configurations, or population like GA, is used similar to the direct simulated annealing (DSA) proposed by Ali et al. [36]. Particle swarm optimization (PSO), which is a relatively new stochastic search algorithm, was first introduced by Kennedy and Eberhart [37] in 1995. It is relatively easier to implement and there are few parameters to adjust [38]. Being easily trapped at local optima and premature convergence are its drawbacks [38,39]. That is why some modifications were introduced in PSO [38,39]. Simulated annealing is very good in escaping from local optima because of the occasional uphill moves, so a hybrid algorithm combining particle swarm optimization and simulated annealing was proposed by Fang et al. [40].

As far as the authors know there is no detailed comparative study of the global search algorithms with regard to their relative effectiveness in composite design optimization; but there are a few comparative studies on other problem areas of structural optimization. For example, Baumann and Kost [41] used three stochastic global search algorithms, SA, GA, and random cost, to find the optimal truss topology having the minimum weight. Starting at different initial configurations, they employed these algorithms each time with a different random sequence and compared relative performances of these algorithms. SA turned out to be the most reliable of the three.

As an alternative approach, lamination parameters [13,15,42–48] are used as optimization variables instead of lamina angles or thicknesses. In this way, the optimization problem becomes convex. In such problems all local optima are globally optimal and local search algorithms can easily find the optimal point. Therefore, the approach is computationally efficient. However, the lamination variables are continuous and their number is often less than the number of design variables (lamina angle and thickness). In order to obtain discrete fiber angles and thicknesses that match the optimal values of the lamination parameters, a second optimization procedure is needed. This second optimization problem is non-convex and non-trivial. In some cases, stochastic search algorithms such as GA need to be used as search algorithm [42–45,48]. However, lamination parameters obtained in the first and the second levels may not be completely matched. If there is a discrepancy between them, optimal lay-up obtained at the second level will be worse than the one obtained at the first level.

Several studies [44–47] adopted lamination parameters as the variables of the response surface approximations. This method reduces the non-linearity of the objective function. Besides, the number of design variables is not increased with the increase in the number of laminae in the laminate. In response surface methods, a polynomial is used to approximate a complex function to reduce computational cost. Therefore, response surface methods cannot give exactly the same representation of a structural system and can lead to errors [46,47].

Objective function of the optimization problem should be accurately calculated during an optimization process to avoid spurious optimum points. Because bending–twisting affects were not accounted for in the laminate analyses of some studies of frequency optimization, the researchers imposed some restrictions on fiber orientations to avoid excessive errors in the frequency results. Bert [1,2] considered balanced laminates, which allowed approximate solution of bending–twisting effects, and Rao and Singh [6] considered cross-ply laminates, which did not have bending–twisting coupling. Narita and Zhao [11] neglected bending–twisting effects in the natural frequency calculation. Abachizadeh and Tahani [17] and Adali and Verijenko [21] neglected the bending–twisting effects but in order to avoid excessive error, they imposed special constraints on bending stiffness terms. These restrictions, however, might prevent from finding much better designs. For this reason, in an effective design optimization, there should be no limitation on fiber orientations except the ones due to manufacturing and design requirements. The method used to evaluate natural frequencies should yield correct results for any arbitrary laminate configuration. Natural frequencies of laminated plates can be calculated via either approximate or exact solution methods. Approximate methods like Rayleigh–Ritz method and finite element method [16,26,27] are capable of accounting for the coupling effect. If the natural frequency is obtained by the traditional analytical approaches like Navier's method, the natural boundary conditions cannot be satisfied in the presence of bending–twisting coupling. The traditional analytical approaches can find the correct solution only for few specific types of stacking sequences that do not involve bending–twisting coupling. By using the boundary-continuous-displacement (BCD) type Fourier series method proposed by Chaudhuri [49], Chaudhuri et al. [50] presented a solution for the free vibration problem of symmetric rectangular anisotropic laminates. In this method, the geometric boundary conditions are satisfied as well as the natural boundary conditions unlike Navier's approach. They obtained a closed form solution valid for all stacking sequences.

The objective of the present study is to find the optimum stacking sequence that gives the maximum natural frequency or maximum frequency separation for fiber–reinforced laminated plates. The BCD-type Fourier series method [49,50] is employed to calculate the natural frequency of the laminated plates. This study is different from the previous ones basically in two aspects: Firstly, it is the first study that used an analytical method accounting for bending–twisting coupling to calculate the frequency response of laminates during optimization. In this way, no restrictions on ply angles need to be imposed to avoid error in calculation. Besides, the accuracy of the approximate methods is questionable and inaccurate calculation of the objective function value may significantly distort its contours and thus change the location of the local extremum points. For that reason, the suitability of the analytical methods not accounting for bending–twisting coupling and approximate methods like Rayleigh–Ritz and finite element methods accounting for this coupling will be tested through the comparison of the results of this study and the previous studies. Secondly, a new version of simulated annealing algorithm is employed for laminated plate optimization.

2. Problem statement

In this study, out-of-plane free vibration response of simply supported rectangular laminated plates (Fig. 1) is considered. The plates are made of stacks of plies symmetrically arranged about the middle surface.

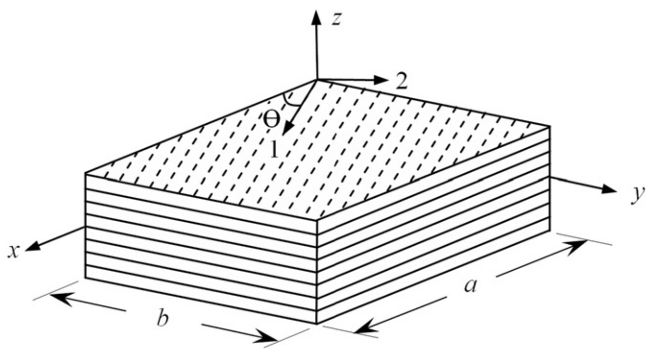

Fig. 1. A rectangular laminated plated consisting of multiple laminae.

Fig. 2. Stacking sequence of a laminate.

Stacking sequence of a symmetric laminate is designated as $[\theta_1/\theta_2/\ldots/\theta_{n-1}/\theta_n]_s$, where θ_1 is the orientation angle of the outermost lamina and θ_n is the innermost lamina below the mid-plane as shown in Fig. 2. The laminae consist of a certain number of plies with a given thickness. The thickness of each lamina is the same and not varied during the optimization. Because the laminate is symmetric, there are n distinct fiber orientation angles, θ_1, θ_2, θ_3, …, θ_n.

In this study, the frequency parameter, Ω, given by Nemeth [51] is used as the objective function.

$$\Omega = \omega a^2 \sqrt{\frac{\overline{\rho}}{D_0}} \tag{1}$$

where ω is the natural frequency, a is the length of the rectangular plate, $\overline{\rho}$ is the mass density of the plate per unit area, D_0 is the reference bending stiffness defined by

$$D_0 = \frac{E_2 h^3}{12(1-\nu_{12}\nu_{21})} \tag{2}$$

where ν is Poisson's ratio, E_2 is the elastic modulus of the lamina transverse to the fiber direction and h is the thickness of the laminate. Instead of D_{ij} ($i,j=1,2,6$), D_o is used in the definition of the frequency parameter because it does not change with the change of fiber orientations. Because frequency is normalized with the laminate thickness, the optimum stacking sequence will be independent of ply thickness.

The first problem is to find the optimum configuration of the composite laminate having the maximum fundamental frequency parameter with a predetermined number of layers. Thus the objective is stated as

$$\text{Minimize} -\Omega_1(\theta_1,\theta_2,\theta_3,\ldots,\theta_n)$$

where $\Omega_1(\theta_1,\theta_2,\theta_3,\ldots,\theta_n) = \text{minimum of } \Omega_{rs}(\theta_1,\theta_2,\theta_3,\ldots,\theta_n)$

$$\text{Subject to } -90 \le \theta_k \le 90 \quad \text{where} \quad k=1,2,\ldots,n$$

Here Ω_i are the frequency parameters corresponding to the natural frequencies ω_i, which are the eigenfrequencies corresponding to the eigenmodes (r,s) and ω_1 is the smallest one, which is called the fundamental frequency. The orientation angles of the fibers in the lower (or upper) layers of the laminate with respect to the mid-plane, θ_k, are the design variables.

The second problem is to find the optimum configuration with maximum separation between two adjacent frequencies, which is called the frequency separation problem.

$$\text{Minimize } -(\Omega_{i+1}(\theta_1,\theta_2,\theta_3,\ldots,\theta_n) - \Omega_i(\theta_1,\theta_2,\theta_3\ldots\theta_n)) \quad i=1,2$$

$$\text{Subject to } -90 \le \theta_k \le 90 \quad \text{where} \quad k=1,2,\ldots,n$$

There are basically two types of laminate configurations that do not involve bending–twisting coupling, i.e. $D_{16}=0$ and $D_{26}=0$; antisymmetric angle-ply laminate and cross-ply laminate. The first one is a laminate having laminae oriented at $+\theta$ to the laminate coordinate axes on one side of the middle surface and corresponding equal-thickness laminae oriented at $-\theta$ on the other side. Because antisymmetric laminates are not symmetric, the coupling stiffness terms, B_{ij}, do not vanish. The second one is a laminate made of a stack of orthotropic laminae whose principal material axes are aligned with the laminate coordinate axes. Other than these two types of laminate configurations, practically there is no general laminate configuration in which bending–twisting coupling does not exist. This means a very limited class of laminates has no bending–twisting coupling. For this reason, the method used for calculating natural frequency should take into account this effect in order to avoid the associated error and the resulting false optimum designs.

3. Methodology

3.1. Natural frequency analysis of laminated plates

The governing differential equation for free vibration of symmetrically laminated plates according to the classical lamination theory is given as

$$D_{11}\frac{\partial^4 w}{\partial x^4}+4D_{16}\frac{\partial^4 w}{\partial x^3\partial y}+2(D_{12}+2D_{66})\frac{\partial^4 w}{\partial x^2\partial y^2}+4D_{26}\frac{\partial^4 w}{\partial x\partial y^3}+D_{22}\frac{\partial^4 w}{\partial y^4}=-\overline{\rho}\frac{\partial^2 w}{\partial t^2} \tag{3}$$

where D_{ij} (i,j=1,2,6) are laminate bending stiffness terms, which are defined in terms of principal stiffness components, Q_{ij}, and ply coordinates (Jones [52]), w is the transverse deflection, $\overline{\rho}$ is the mass density of the plate material per unit area, and t is time. The boundary conditions for simply supported edges are given as follows

$$w=0 \quad \text{and} \quad M_x=-\left(D_{11}\frac{\partial^2 w}{\partial x^2}+2D_{16}\frac{\partial^2 w}{\partial x\partial y}+D_{12}\frac{\partial^2 w}{\partial y^2}\right)=0 \quad \text{for} \quad x=0,a \tag{4}$$

$$w=0 \quad \text{and} \quad M_y=-\left(D_{12}\frac{\partial^2 w}{\partial x^2}+2D_{26}\frac{\partial^2 w}{\partial x\partial y}+D_{22}\frac{\partial^2 w}{\partial y^2}\right)=0 \quad \text{for} \quad y=0,b \tag{5}$$

where M_x and M_y are the bending moment resultants on the x and y faces and a and b are the length and the width of the rectangular plate.

BCD—double Fourier series method (Chaudhuri [49]) was employed to solve the governing differential equation for natural frequencies of rectangular thin laminated plates. Considering the natural frequency problem of arbitrarily laminated plates, it is not possible to satisfy all the boundary conditions and establish a solution with the general continuous Fourier series. However, if proper discontinuities are added to the assumed solution function and its derivatives at the boundaries, all of the boundary conditions can be satisfied and a solution can be obtained. The coupled partial differential equation of motion is reduced to the following set of equations [50]:

$$\sum_{m=1}^{\infty}\sum_{n=1}^{\infty}\{P_{mn}^{rs}-\lambda\delta_{mn}^{rs}\}W_{mn}=0 \tag{6}$$

$$P_{mn}^{rs}=\begin{cases} Q_{mn}^{rs}h_{mn}^{rs}, & m+r=\text{odd}, \qquad n+s=\text{odd};\\ 0, & m+r=\text{even}, \quad \text{or} \quad n+s=\text{even}; \end{cases} \tag{7}$$

$$P_{mn}^{rs}=\alpha_r^4+2\zeta\alpha_r^2\beta_s^2+\eta\beta_s^4 \tag{8}$$

$$Q_{mn}^{rs}=-2\alpha_m\beta_n\{\gamma({\alpha_m}^2+{\alpha_r}^2)+\chi({\beta_s}^2+{\beta_n}^2)\} \tag{9}$$

$$h_{mn}^{rs}=h_{rm}h_{sn} \tag{10}$$

$$\delta_{mn}^{rs}=\begin{cases} 1, & m=r, \quad n=s;\\ 0, & \text{otherwise} \end{cases} \tag{11}$$

$$\alpha_r=\frac{r\pi}{a}, \quad \beta_s=\frac{s\pi}{b} \tag{12}$$

$$\zeta=\frac{(D_{12}+2D_{66})}{D_{11}}, \quad \eta=\frac{D_{22}}{D_{11}}, \quad \lambda=\frac{\overline{\rho}\omega^2}{D_{11}}, \quad \gamma=\frac{D_{16}}{D_{11}}, \quad \chi=\frac{D_{26}}{D_{11}} \tag{13}$$

$$h_{\rm rm}=\begin{cases} \frac{4m}{\pi(m^2-r^2)}, & m+r=\text{odd}\\ 0, & m+r=\text{even} \end{cases}, \quad h_{\rm sn}=\begin{cases} \frac{4n}{\pi(n^2-s^2)}, & n+s=\text{odd}\\ 0, & n+s=\text{even} \end{cases} \tag{14}$$

where m, n, r, s are the indices of the Fourier series, W_{mn} are the plate Fourier coefficients, ω is the natural frequency of the laminate.

Expanding Eq. (6) with a certain number of terms in Fourier series leads to a system of equations, which may be expressed in matrix form. The size of this matrix depends on the number of the terms taken from the Fourier series. Eigenvalues corresponding to different modes can be found by setting the determinant of this matrix to zero. Fundamental frequency, which is the lowest of all the natural frequencies, always corresponds to the eigenmode (r,s) being equal to (1,1).

Table 1
Material properties for graphite–epoxy [8,53,54].

E_{11}	138 GPa
E_{22}	8.96 GPa
G_{12}	7.1 GPa
υ_{12}	0.3

Table 2
Comparison of the frequency parameter values for [30]*T* with $a=b$.

	Mode					
	1	2	3	4	5	6
Present (8 terms)	11.689	21.002	33.909	35.617	48.723	49.779
Present (20 terms)	11.447	20.597	33.368	35.205	47.841	48.870
Reference [53] (8 terms)	11.264	20.307	33.000	34.920	47.247	48.353
Reference [54] (8 terms)	11.69	21.00	33.91	35.62	48.72	49.78

3.2. Testing the convergence of the method

In this study, convergence tests were conducted to determine how many Fourier series terms were sufficient to obtain the desired accuracy. In the convergence tests, the material properties (Table 1) and the laminate configurations given by Narita [8], Cupial [53] and Leissa and Narita [54] were used.

Narita [8] considered a rectangular eight-layered plate with a symmetric lay-up, $[45/-45_3]_s$, and an aspect ratio being equal to one. If 20 terms are used in the Fourier series, the value that the BCD-double Fourier series method yields for this laminate configuration is 56.334 for the frequency parameter. If 30 terms are used, the value becomes 56.329.

Cupial [53] and Leissa and Narita [54] considered a rectangular 30° one-layered plate with an aspect ratio of one. For this laminate configuration, the BCD-double Fourier series method gives 11.447 and 11.381 with 20 and 30 terms respectively.

For the chosen laminate configurations, the frequency parameter takes stable values if 10–20 terms are included. Accordingly, the natural frequency calculations were carried out with the first 20 terms of the Fourier series.

3.3. Comparison of the frequency analysis results

The results of the analytical frequency model used in this study in terms of frequency parameter (Eq. (1)) were compared with the ones obtained in previous studies. Table 2 shows the frequency parameters corresponding to the first six modes calculated with 8 and 20 terms of the Fourier series for the same material properties and laminate lay-up as in the previous problem. In both of the studies [53,54] referred in Table 2, Rayleigh–Ritz method was used with 8×8 polynomials including bending–twisting effects. As seen in the table, the results obtained by the frequency analysis used in this study are close to the results provided in the literature.

3.4. Optimization method

In the present study, in order to search for the globally optimum laminate designs, a variant of simulated annealing (SA) algorithm is proposed. There are similarities to the direct simulated annealing (DSA) proposed by Ali et al. [36]; but many of its features were modified to improve the reliability and efficiency.

DSA uses a set of current configurations, or population, rather than a single current configuration as in the SA algorithm. In this way, unlike the standard SA algorithm, where only the neighborhood of a single point is searched, DSA searches the neighborhood of all the current points in the set. If a new configuration is accepted, it substitutes the worst current configuration so the good configurations are always kept in the set unless better ones are found. In ordinary simulated annealing, many good configurations are lost when they are replaced by worse configurations especially at the early stages of optimization. .

Firstly, N configurations are randomly created at the beginning of the optimization process. N depends on the dimension of the problem, n, i.e. number of design variables. In the present problem, the dimension, n, is equal to the number of distinct fiber angles. Since the laminate is symmetric, n is actually equal to the half of the total number of laminae. Ali et al. [36] tested the algorithm for different configuration numbers such as N being equal to $5(n+1)$ $7(n+1)$, $10(n+1)$ and compared the number of function evaluations, number of failures and computational times. The reliability of the algorithm increases with the increased number of current configurations, N, at the expense of computational time. In the case that the number of N is high, many current configurations will be dispersed all over the solution domain at high temperatures. Because search is conducted in the neighborhood of the current configurations, this will enable thorough search of the solution domain and thus increase the probability of finding the globally optimum point. However, convergence takes a long time with many current configurations because all the current configurations should gather around the best found optimum point during the optimization process. Therefore, increasing N improves reliability at the expense of efficiency. On the other hand, if the number of N is low, the solution domain may not be thoroughly searched with a few current configurations. This will reduce the chances of finding the global optimum. In this study, the number of current configurations was chosen as

$$N = 8\ (n+1) \tag{15}$$

The initial configurations are generated by randomly choosing lamina angles, θ_k, between -90° and 90°. Because fiber orientation angles should be discrete due to manufacturing requirements, generated angle values are rounded to the closest chosen discrete angle. The designer decides on the angle increments, which may be 30°, 15°, 10°, 5°, 1° or even less, according to the manufacturing precision or ease of application.

In each iteration, a new configuration is randomly generated in the neighborhood of a current configuration. This is achieved by first randomly choosing one of the current configurations and then introducing random variations to its lamina angles. The new lamina angle of the kth layer, θ'_k, is calculated as

$$\theta'_k = \theta_k + r\,\Delta\theta_{\max} \tag{16}$$

where r is a randomly chosen real number between -1.0 and 1.0 ($r \in \Re : -1 \le r \le 1$), θ_k is the current angle of the kth lamina, and $\Delta\theta_{\max}$ is the maximum angle variation. If the angles fall outside of the interval ($-90 \le \theta'_k \le 90$), they are modified according to

$$\theta''_k = \left\{ \begin{array}{ll} \theta'_k - 180 & \text{if} \quad \theta'_k > 90 \\ \theta'_k + 180 & \text{if} \quad \theta'_k < -90 \\ \theta'_k & \text{if} \quad -90 \le \theta'_k \le 90 \end{array} \right\} \tag{17}$$

where θ''_k is the modified angle value.

When a new configuration is generated, its objective function value, which is either $-\Omega_1$ or $-(\Omega_{i+1}-\Omega_i)$, is calculated. The minus sign, "$-$" is introduced, because the optimization problem is formulated as a minimization problem. The new trial configuration is either accepted or rejected according to the acceptance criterion of the simulated annealing algorithm. Acceptability is based on the following formula:

$$A_t = \left\{ \begin{array}{ll} 1 & \text{if} \quad f_t \le f_h \\ \exp(-(f_t - f_h)/T_k) & \text{if} \quad f_t > f_h \end{array} \right\} \tag{18}$$

where f_t is the cost of the trial design, f_h is the cost of one of the high-cost current configurations; T_k is the temperature parameter for the kth Markov chain. A Markov chain is a sequence of trials accomplished at the same temperature. If A_t is greater than a number, P_r, generated randomly between 0.0 and 1.0, then the new configuration is accepted, otherwise it is rejected. A_t is compared with a random number instead of a constant number like 0.5 in order to allow large uphill moves by occasionally accepting quite worse configurations so that the algorithm may escape local minimum points. According to Eq. (18), the trial designs that are better than the worst current design are always accepted. As the formula implies, the acceptability of newly generated configurations, A_t, is high at high temperatures. It decreases with the decreasing temperature and in the end worse designs are almost never accepted.

The temperature parameter, T, controls the convergence of the optimization process just like the temperature controls micro-structural changes in the physical annealing process. At the beginning of the algorithm, the temperature parameter must be relatively high. This is because the probability of acceptability must be high in order to prevent getting stuck into a local minimum at early stages of the optimization and search a large design space. This stage resembles melting in the physical annealing where atoms can rearrange themselves freely. During optimization, the temperature is lowered in order to converge on a local optimum. The temperature parameter should be decreased gradually so that a large part of the solution domain can be searched without getting stuck to a local minimum. This is like slow cooling down of metals where time and temperature driven micro-structural changes occur. At the final stages, it should take such low values that a new configuration that is worse than the current configurations is almost never accepted. This corresponds to the freezing stage where atom rearrangements stabilize. The temperature in the kth Markov chain is calculated as

$$T_k = \alpha_k T_{k-1} \tag{19}$$

where T_{k-1} is the temperature parameter in the $(k-1)$th Markov chain and α_k is temperature reduction factor.

In DSA, if a new configuration is accepted, it replaces the worst configuration. The replacement scheme of DSA has one drawback that becomes especially apparent in problems with a large number of design variables. For instance, if one optimizes a laminate with 16 distinct lamina angles using DSA, the number of current configurations will be $8(16+1)=136$. The current configurations other than the worst one are never replaced unless better ones are found. At the initial stages of the optimization process, they quickly gather around local minimums when the high-cost initial configurations are replaced by better new configurations. The worst one, on the other hand, is continued to be frequently updated, because it can be replaced by higher-cost configurations and can be anywhere within the solution domain at high temperatures. Because new configurations are generated in the neighborhood of the current ones, search becomes restricted to a small segment of the feasible domain where current configurations are concentrated except for the trials in which the new configuration is generated around the worst current configuration, which are very infrequent. In order to remedy this, the replacement scheme of DSA was modified. The current configurations are ordered with respect to their objective function value. If a new configuration is accepted, it replaces a current configuration randomly chosen among $(n+1)$ worst configurations instead of the worst one. Thus, $7(n+1)$ of the current configurations having low cost remain in the set unless better ones are found through iterations. These may be concentrated around local optimums. The others, on the other hand, may be replaced by higher cost configurations with a probability depending on the temperature parameter. In this way, $(n+1)$ configurations become dispersed all over the feasible domain at high temperatures. Whenever one of them is chosen, a new configuration is generated in its neighborhood. This means that search can be conducted in almost any part of the solution domain and thus a more thorough search of the feasible domain can be achieved. In the modified version of the algorithm, the objective function value of the best of the worst $(n+1)$ current configurations is used for f_h in Eq. (18).

Another issue in reliable global search is that the algorithm should be able to search a large solution domain. In order to ensure this, instead of giving small perturbations to the current configuration to obtain a new configuration in its near neighborhood, one should allow a large variance in the current configurations. Considering that the current configurations are scattered over the solution domain at the initial stages of the optimization process, a new configuration can be generated at any point within the solution domain if a large variation is allowed. For the present problem, a large value (50°) is chosen for the maximum angle variation, $\Delta\theta_{\max}$ in Eq. (16), at the beginning of the optimization. This means that at initial stages, the neighborhood of the current configurations, where a better configuration is searched, is large. In this way, the solution domain can thoroughly be searched. With the progression of optimization, improvements in the current configurations become scarce. If large variation is continued, improvements will be quite rare and convergence will take quite a long time. For this reason, if there is no improvement in the worst of the best $7(n+1)$ current configurations during a Markov chain, $\Delta\theta_{\max}$ is reduced by multiplying with a factor, c, to make the searched region smaller and thus increase the likelihood of finding a better design.

$$\Delta\theta'_{\max} = c\Delta\theta_{\max} \tag{20}$$

Toward the end of the optimization process, only close neighborhood of the current configurations is searched in order to exactly determine the optimal point. This is similar to the physical annealing process. At the beginning, when the temperature is high, atoms disorderly move around and their mobility is so high that they are able to move large distances. During cool down, the movements of the atoms become slow so they can make only small-scale arrangements. Temperature controls the mobility of the atoms; this in turn affects the potential arrangements of the atoms. In a similar way, $\Delta\theta_{\max}$, the maximum variation in the optimization variables, affects the search process by controlling the scale of variation in the current designs.

In another respect, $\Delta\theta_{\max}$ plays a role similar to that of temperature in physical annealing processes. Reduction in the temperature should be slow enough to allow time-dependent micro-structural changes to occur and to reach equilibrium. In simulated annealing, iterations need to be continued in a Markow chain until equilibrium is reached. Non-improvement in the current best $7(n+1)$ configurations during a Markow chain implies that further changes are unlikely with the current value of $\Delta\theta_{\max}$ and thus equilibrium is reached. Because this gives a clear-cut measure, $\Delta\theta_{\max}$ is a better indication of equilibrium at a specific temperature level. For this reason, the reduction scheme for the temperature parameter in the original DSA algorithm is not adopted; instead it is made dependent on the reduction in $\Delta\theta_{\max}$ (the factor, c, in Eq. (20)). The temperature reduction factor, α_k in Eq. (19), is calculated as

$$\alpha_j = \begin{cases} \alpha_{\max} & \text{if} \quad L_a^j/L^j < [(\Delta\theta_{\max})/(\Delta\theta_{\text{imax}})]^2 + 0.01 \\ \alpha_{\min} & \text{else} \end{cases} \tag{21}$$

where L^j is the number of trials executed in the jth Markow chain and L_a^j is the number of accepted configurations. Accordingly, L_a^j/L^j ratio is a measure of acceptability in a Markow chain, $\Delta\theta_{\text{imax}}$ is the initial maximum variation in the lamina angles. $\alpha_{\max}$ and $\alpha_{\min}$ are chosen to be 0.9999 and 0.99. If the acceptance ratio becomes smaller than the square of $\Delta\theta_{\max}/\Delta\theta_{i\max}$ ratio due to reduction in $\Delta\theta_{\max}$, temperature is reduced at a higher rate by multiplying with $\alpha_{\min}$. At the initial stages of the optimization, the right hand side of the inequality is close to 1.0; accordingly, the temperature level is kept high such that the ratio of the number of accepted trials to the total number of trials is close to 1.0. When $\Delta\theta_{\max}$ approaches zero at the end of the optimization process, temperature parameter also approaches zero; acceptability of a new configuration, A_t in Eq. (18), then becomes close to zero. Iterations are continued until the difference between the values of the best and the worst current configurations becomes small.

One of the disadvantages of the global search algorithms is that many parameters should be tuned when they are applied to a different problem. Otherwise, the expected performance cannot be achieved. Finding suitable values, on the other hand, requires extensive numerical experiments. In this respect, the application of the present algorithm to a different problem is much easier. Suitable values for most of the parameters can be found without difficulty. The initial value of the temperature parameter, T, in Eq. (18) is chosen so high that almost all of the randomly generated configurations are accepted; but unlike the other variants, choosing a value much higher value than necessary does not affect the number iterations executed during the optimization process. This is because the reduction in the temperature parameter is made dependent on the reduction in $\Delta\theta_{max}$ through Eq. (21). If the temperature parameter has a very high value, it is quickly reduced to the levels that will yield the required acceptability ratio, L_a^j/L^j. The initial value of the maximum variation that may be introduced to the optimization variables, $\Delta\theta_{imax}$, is another parameter affecting convergence. Its value is chosen based on the extent of the solution domain. Its value should be chosen as high as possible in order to search the solution domain thoroughly. For the present problem, the initial value of $\Delta\theta_{max}$ is chosen as 50°, knowing that the upper and lower limits of θ are 90° and −90°. The value of factor c in Eq. (20) depends on the difficultly of the problem. The higher the number, the more iterations are executed. If the number of variables is four or less than four, 0.9 is a suitable value. If the number of variables is 16 or more, a much slower reduction in the maximum variation is required; a number as high as 0.999 permits a thorough search of the solution domain. The only parameter that requires numerical experiments to determine its value is then c.

4. Results and discussion

4.1. Comparison of the optimization results for frequency separation

Adali and Verijenko [21] considered problems of separation between the first and the second frequencies and between the second and the third frequencies. They optimized symmetric laminates having 4, 8, 12 and 16 plies with an aspect ratio of 2.0. Each symmetric ply pair might have a different fiber angle. Up to eight different fiber angles were used as design variables. These angles might take only four different discrete values {0°, −45°, 45°, 90°}. They used T300/5280 graphite–epoxy and Scotchply 1002 glass–epoxy. Their optimization results and the results of the present study are given in Tables 3–5. $\Delta\Omega_{ij}$ is the difference between the frequency parameters Ω_i and Ω_j corresponding to natural frequencies ω_i and ω_j as defined in Eq. (1). All the values of the frequency parameter, Ω, given in the table were calculated by the analytical method used in this study. While the optimum lay-up configuration did not change for glass–epoxy with increased number of distinct fiber orientations (Table 3), frequency separation is greatly improved for graphite–epoxy (Tables 4 and 5). Adali and Verijenko [21] neglected the bending–twisting effects for simplicity and imposed special constraints on bending stiffness terms to avoid excessive error. In this study, bending–twisting effects were not neglected so these constraints were not used. However, the same optimum designs were found for glass–epoxy (Table 3), which did not involve bending–twisting coupling. On the other hand, the results for graphite–epoxy (Tables 4 and 5) show some differences. Since they used enumeration as the optimization method, the discrepancy may not be attributed to differences in the search algorithms, but to the constraints that they used for bending–twisting coupling.

4.2. Results of frequency separation for different design domains

When the number of design variables or the range of values that they may take is increased the design space gets larger, i.e. the number of configurations that the search algorithm may try increases. It is very likely that the enlarged design domain includes a better design. Accordingly, one may obtain improvement in the optimal design by choosing a larger design domain. However, existence of a larger number of local optimums in a larger domain causes difficulties in locating the globally optimum configuration. This requires use of a reliable global search algorithm like SA.

Table 3
Optimum angles for frequency separation $\Delta\Omega_{12}$ for glass–epoxy with an aspect ratio of 2.0.

Number of plies	Optimum design reference [21]	Optimum design present	Ω_1 and Ω_2 present	$\Delta\Omega_{12}$ present
4	$[0_2]_s$	$[0_2]_s$	$\Omega_1=54.63$, $\Omega_2=112.78$	58.15
8	$[0_4]_s$	$[0_4]_s$	$\Omega_1=54.63$, $\Omega_2=112.78$	58.15
12	$[0_6]_s$	$[0_6]_s$	$\Omega_1=54.63$, $\Omega_2=112.78$	58.15
16	$[0_8]_s$	$[0_8]_s$	$\Omega_1=54.63$, $\Omega_2=112.78$	58.15

Table 4
Optimum angles for frequency separation $\Delta\Omega_{12}$ for graphite–epoxy with an aspect ratio of 2.0.

Number of plies	Optimum design reference [21]	Ω_1 , Ω_2 and $\Delta\Omega_{12}$	Optimum design present	Ω_1 , Ω_2 and $\Delta\Omega_{12}$ present
4	$[0/45]_s$	$\Omega_1=78.72$, $\Omega_2=188.45$ $\Delta\Omega_{12}=109.73$	$[0_2]_s$	$\Omega_1=67.59$, $\Omega_2=178.44$, $\Delta\Omega_{12}=110.85$
8	$[0_3/45]_s$		$[0_3/45]_s$	$\Omega_1=69.23$, $\Omega_2=183.84$, $\Delta\Omega_{12}=114.61$
12	$[0_4/45/0]_s$	$\Omega_1=79.90$, $\Omega_2=185.54$, $\Delta\Omega_{12}=114.64$	$[0_5/90]_s$	$\Omega_1=68.42$, $\Omega_2=183.71$, $\Delta\Omega_{12}=115.29$
16	$[0_6/45/90]_s$		$[0_6/45/90]_s$	$\Omega_1=69.38$, $\Omega_2=184.75$, $\Delta\Omega_{12}=115.37$

Table 5
Optimum angles for frequency separation $\Delta\Omega_{23}$ for graphite–epoxy with an aspect ratio of 2.0.

Number of plies	Optimum design reference [21]	Ω_2, Ω_3 and $\Delta\Omega_{23}$	Optimum design present	Ω_2, Ω_3 and $\Delta\Omega_{23}$ present
4	$[0/90]_s$	$\Omega_2=184.77$, $\Omega_3=288.62$, $\Delta\Omega_{23}=103.85$	$[-45/45]_s$	$\Omega_2=208.90$, $\Omega_3=320.49$, $\Delta\Omega_{23}=111.59$
8	$[0/90/0_2]_s$		$[0/90/0_2]_s$	$\Omega_2=184.77$, $\Omega_3=347.48$, $\Delta\Omega_{23}=162.71$
12	$[0_2/90/-45/90_2]_s$	$\Omega_2=189.61$, $\Omega_3=357.81$, $\Delta\Omega_{23}=168.20$	$[0_2/90/45/90/0]_s$	$\Omega_2=189.60$, $\Omega_3=358.23$, $\Delta\Omega_{23}=168.63$
16	$[0_3/90_3/-45/0]_s$, $[0_3/90_3/0_2]_s$	$\Omega_2=184.77$, $\Omega_3=354.84$, $\Delta\Omega_{23}=170.07$	$[0_3/90_3/-45/0]_s$	$\Omega_2=185.63$, $\Omega_3=357.45$, $\Delta\Omega_{23}=171.82$

Table 6
Optimum lamina angles for the lay-up configuration $[\alpha_8\ /\ \beta_8\ ]_s$ with different discrete angle increments for maximum frequency separation.

Angle increment	Optimum design $[\alpha_8/\beta_8]_s$	Frequency parameter, Ω		
		1. Mode	2. Mode	Difference
90°	$[0_8/90_8]_s$	49.160	111.711	62.551
45°	$[0_8/90_8]_s$	49.160	111.711	62.551
30°	$[30_8/-60_8]_s$	58.556	125.551	66.995
15°	$[30_8/-60_8]_s$	58.556	125.551	66.995
10°	$[20_8/-80_8]_s$	53.198	120.334	67.136
5°	$[25_8/-70_8]_s$	55.959	123.630	67.671
1°	$[25_8/-72_8]_s$	55.734	123.441	67.707

Table 7
Optimum lamina angles for the lay-up configuration $[\alpha_4/\beta_4/\gamma_4/\theta_4]_s$ with different discrete angle increments for maximum frequency separation.

Angle increment	Optimum design $[\alpha_4/\beta_4/\gamma_4/\theta_4]_s$	Frequency parameter, Ω		
		1. Mode	2. Mode	Difference
90°	$[0_4/90_4/0_8]_s$	51.726	142.260	90.534
45°	$[0_4/90_4/0_4/-45_4]_s$	52.093	142.739	90.646
30°	$[0_4/90_4/0_4/-30_4]_s$	51.974	142.666	90.692
15°	$[0_4/90_4/0_4/-30_4]_s$	51.974	142.666	90.692
10°	$[0_4/90_4/0_4/-30_4]_s$	51.974	142.666	90.692
5°	$[0_4/90_4/5_4/-35_4]_s$	52.094	143.087	90.993
1°	$[-1_4/90_4/1_4/35_4]_s$	52.045	143.108	91.063

In order to see the possible improvements in this respect, the number of distinct fiber angles and the range of values they may take were increased. Frequency separation problem for a 32-ply laminate with an aspect ratio of 1.2 was considered. Material properties given in Table 1 were used for the laminate. Firstly, a laminate configuration with two distinct lamina angles, $[\alpha_8/\beta_8]_s$, was optimized. This is a symmetric laminate with four laminae each made of a stack of eight plies. Table 6 presents the results for different angle increments. An angle increment of 5° means that the possible fiber angles are $-90°$, $-85°$, ..., $-5°$, 0°, 5°, ..., 85°, 90°. The results indicate that when the angle increment is decreased, i.e. the range of values that the design variables may take is increased, a better optimal design with a larger frequency separation is obtained.

Then, laminates with four and eight distinct lamina angles ($[\alpha_4/\beta_4/\gamma_4/\theta_4]_s$ and $[\alpha_2/\beta_2/\gamma_2/\theta_2/\xi_2/\tau_2/\phi_2/\psi_2]_s$) were considered. Tables 7 and 8 show the optimum designs. Since stacking sequence is important for out-of-plane deformation, only the adjacent plies are shown by a single symbol, e.g. $[90/90/90/0/0/0/90/0]_s$ is shown as $[90_3/0_3/90/0]_s$ not as $[90_4/0_4]_s$, because they have different natural frequencies for out-of-plane vibration.

As seen in the tables, with increasing number of design variables, i.e. number of lamina angles, a larger separation in frequency is obtained. Increasing the number from two to four resulted in an improvement of about 35% to 45%. With eight distinct angles, a larger frequency separation can be obtained even with a limited number of permissible angles like {−90°, 0°, 90°}. Further

Table 8
Optimum lamina angles for the lay-up configuration $[\alpha_2/\beta_2/\gamma_2/\theta_2/\xi_2/\tau_2/\varphi_2/\psi_2]_s$ with different discrete angle increments for maximum frequency separation.

Angle increment	Optimum design $[\alpha_2/\beta_2/\gamma_2/\theta_2/\xi_2/\tau_2/\varphi_2/\psi_2]_s$	Frequency parameter, Ω		
		1. Mode	2. Mode	Difference
90°	$[0_2/90_2/0_6/90_6]_s$ $[0_4/90_2/0_2/90_6/0_2]_s$	51.783	142.878	91.096
45°	Same as above	51.783	142.878	91.096
30°	Same as above	51.783	142.878	91.096
15°	Same as above	51.783	142.878	91.096
10°	Same as above	51.783	142.878	91.096
5°	Same as above	51.783	142.878	91.096
1°	$[0_4/90_2/0_2/90_2/89_2/90_2/-28_2]_s$	51.818	142.949	91.133

Table 9
Optimum lamina angles for 16 distinct laminae for maximum frequency separation.

Angle increment	Optimum design 16 distinct lamina angles	Frequency parameter 1. Mode	Frequency parameter 2. Mode	Frequency parameter difference
90°	$[0_5/90_6/0_2/90_3]_s$, $[0_4/90_2/0_2/90_6/0/90]_s$, $[0_5/90_5/0/90_3/0/90]_s$, $[0_3/90/0_2/90/0/90_5/0/90_2]_s$, $[0_3/90/0/90/0/90/0_2/90_6]_s$, $[0_4/90/0/90_3/0/90_2/0/90_3]_s$	51.786	142.917	91.131
45°	Same as above	51.786	142.917	91.131
30°	Same as above	51.786	142.917	91.131
15°	Same as above	51.786	142.917	91.131
10°	Same as above	51.786	142.917	91.131
5°	Same as above	51.786	142.917	91.131
1°	$[0_3/-89/89/90/0_3/-1/0_2/85/-1_3]_s$	51.797	142.935	91.138

Table 10
The optimum laminate designs for maximum frequency separation satisfying the contiguity constraint, i.e. no lamina may contain more than four plies, and the constraint that the difference between two consecutive laminae may not exceed 45°.

Angle increment	Optimum design 16 distinct lamina angles	Frequency parameter 1. Mode	Frequency parameter 2. Mode	Frequency parameter difference
45°	$[0_2/45/0_2/-45/90_2/-45/90_3/-45_2/0/45]_s$	56.353	146.220	89.867
30°	$[0_2/30/0/-30/-60/90/60/90/-60/90/60/30_2/0/30]_s$	57.129	146.831	89.702
15°	$[0_2/15/0/-15/-60/90_2/75_3/90/75_2/-60/-30]_s$	54.318	144.751	90.433
10°	$[0_2/10/0/-20/-60/80_4/90/80/70/80/60/80]_s$	54.302	144.727	90.424
5°	$[0/5_3/-15/-60/85_2/80/85_2/90/85/65/40/35]_s$	53.727	144.321	90.594
1°	$[4/5/0/5/-14/-59/83/85_2/81/88/85/89/80/82/-75]_s$	53.642	144.259	90.617

improvement in the optimum design can be obtained by increasing the number of distinct lamina angles to 16 as shown in Table 9.

4.3. Optimum designs with contiguity and angle difference constraints

In laminate design, a limit is set to the number of contiguous plies of the same orientation to prevent matrix damage propagation and thus avoid large matrix cracks; the maximum thickness is experimentally determined and it is usually taken as four plies for CFRP laminates [56]. Besides, in order to reduce edge delaminations, the difference between the angles of two consecutive laminae should not exceed 45° [56]. These requirements can be taken into account in the present optimization procedure by imposing constraints and adding penalty values to the objective function whenever these constraints are violated. For this purpose, whenever a new configuration is generated, these requirements are checked; if the difference between the fiber angles of two consecutive laminae, $\Delta\theta$, is greater 45°, a penalty value equal to $\Delta\theta-45$ is added. If the number of consecutive plies with the same orientation, s_i, is larger than four, a penalty value equal to $10(s_i-4)$ is added. If the difference between the fiber angles of consecutive laminae is less than 5°, the sum of the number of plies in those laminae is also constrained not to exceed four. With these constraints, frequency difference was maximized using 16 distinct lamina angles. Table 10 presents the results for different angle increments. In comparison to the results presented in Table 9, the results are slightly worse, but satisfy the constraints.

4.4. Natural frequency maximization considering uncertainty in fiber angles

During manufacturing of a laminated plate, orientation angles of the fibers cannot be made exactly the same as the ones specified by the designer. According to the precision of the manufacturing method, fiber angles show some variation, or uncertainty. The value of the objective function used in the design optimization will also show a variation. If the design optimization is carried out by minimizing the worst value of the objective function that may occur due to uncertainty in the angles rather than its value corresponding to the mean values of the fiber angles as in the previous sections, the resulting optimum design might be different. In this section, the impact of taking fiber angles as random variables on the resulting optimum design is explored.

The frequency parameter is a function of the fiber orientation angles as

$$\Omega = g(\theta_1, \theta_2, \ldots, \theta_n) \tag{22}$$

This relation is determined by the analytical method proposed by Chaudhuri et al. [50]. The angles, θ_i, are considered to be independent random variables, i.e. uncertainty in a lamina angle does not depend on the uncertainty of the other. They are taken to be normally distributed with known values of mean, $\mu_{\theta i}$, and variance, $\mathrm{Var}(\theta)$, which is assumed to be the same for all lamina angles, θ_i. Their standard deviation, σ_θ, is the square root of their variance, $\mathrm{Var}(\theta)$. The frequency parameter, Ω, is a response variable whose mean, μ_Ω, and variance, $\mathrm{Var}(\Omega)$, depend on $\mu_{\theta i}$ and $\mathrm{Var}(\theta)$.

The objective is to maximize the fundamental frequency. One may find the optimum angles that produce the maximum frequency. However, because of the variation in the fiber angles, in practice lower values are obtained for the fundamental frequency. In that case, the quality of the design is better judged based the worst value of the fundamental frequency. Considering that frequency is normally distributed, the worst value can be taken as the average value minus three times the standard deviation. The optimization problem now becomes maximizing the worst value instead of the average value of the frequency parameter, Ω. The objective function is then stated as

$$\text{Minimize} - (\mu_\Omega - 3\sigma_\Omega) \tag{23}$$

In order to calculate the objective function, the numerical values of average, μ_Ω, and the standard deviation, σ_Ω, of the frequency parameter need to be obtained. In this study, the average value of Ω, is assumed to be approximately equal to the value of function g in Eq. (22) calculated using the mean values of the angles. Then,

$$\mu_\Omega \cong g(\mu_{\theta_1}, \mu_{\theta_2}, \ldots, \mu_{\theta_n}) \tag{24}$$

Variation of the response variable, $\mathrm{Var}(\Omega)$, can be shown [57] to be approximately equal to

$$\mathrm{Var}(\Omega) \cong \sum_{i=1}^{n} \left(\frac{\partial g}{\partial \theta_i}\right)^2 \mathrm{Var}(\theta) \tag{25}$$

where derivatives $\partial g/\partial \theta_i$ are calculated at the mean values of the angles, θ_i. Because of the difficulty of analytically taking the derivatives, fourth – order backward difference formula is used as given below.

$$\frac{\partial g}{\partial \theta_i} = \frac{-g_{i-3} + 6g_{i-2} - 18g_{i-1} + 10g_i + 3g_{i+1}}{12\sigma_\theta} \tag{26}$$

where g_{i+m} is defined as

$$g_{i+m} = g(\mu_{\theta_1}, \mu_{\theta_2}, \ldots, (\mu_{\theta_i} + m\sigma_\theta), \ldots, \mu_{\theta_n}) \tag{27}$$

Substituting Eq. (26) into Eq. (25), and knowing that $\mathrm{Var}(\theta) = \sigma_\theta^2$, one obtains

$$\mathrm{Var}(\Omega) \cong \sum_{i=1}^{n} \left(\frac{-g_{i-3} + 6g_{i-2} - 18g_{i-1} + 10g_i + 3g_{i+1}}{12}\right)^2 \tag{28}$$

In order to validate Eqs. (24) and (28), normally distributed random values are generated for fiber angles with given average values μ_{θ_i} and standard deviation σ_θ. For this purpose, random numbers between -50 and 50 were generated, then they are multiplied by the probability distribution function (PDF) of the normal distribution with zero mean and the chosen value for σ_θ, which was 3°. If the number is not greater than a randomly generated number between 0 and 1, new random numbers are generated until this condition is satisfied. Then, these random numbers are added to the chosen average values of fiber angles, μ_{θ_i}. After normally distributed random angles, θ_i, were obtained, the corresponding frequency parameter, Ω, was calculated. This process was repeated 10,000 times and the average, μ_Ω, and standard deviation, σ_Ω, of Ω were calculated based on the generated data. Then, they were compared with the values obtained by the fourth order finite difference formula. The difference was turned out to be less than 0.01% for the average, μ_Ω, and less than 2% for the standard deviation, σ_Ω. Use of the backward or forward difference made almost no difference.

After validating Eqs. (24) and (28), the laminate configuration defined by four distinct fiber angles showing uncertainty, $[\alpha/\beta/\gamma/\theta]_s$, was optimized to obtain the maximum fundamental frequency based on its worst value given in Eq. (23). The material properties of AS/3501 graphite–epoxy given in Table 1 were used in the frequency analysis. Table 11 presents the results for natural frequency maximization with different angle increments. It was observed that highly different optimal designs were obtained when the geometry of the plate, i.e. its aspect ratio, was changed. When there is an uncertainty in

Table 11
Optimum lamina angles of laminate configuration $[\alpha/\beta/\gamma/\theta]_s$ for maximum fundamental frequency. Fiber angles are treated as random variables with standard deviation σ_θ. μ_Ω and σ_Ω are the average and the standard deviation of the frequency parameter, Ω.

a/b	σ_θ	Optimum layup	μ_Ω	σ_Ω
1.3	0°	$[-56/54_3]_s$	76.2750	0
	1°	$[-56/54_3]_s$	76.2750	0.0056
	3°	$[-56/54_2/55]_s$	76.2748	0.01670
	5°	$[-56/54_2/55]_s$	76.2748	0.02810
1.5	0°	$[-67/63_3]_s$	93.8927	0
	1°	$[-67/63_2/62]_s$	93.8927	0.0026
	3°	$[-67/63_2/62]_s$	93.8927	0.0077
	5°	$[-67/63_2/62]_s$	93.8927	0.0130

the fiber angles, a different optimal design is obtained. However, the sensitivity of the natural frequency to uncertainty in fiber angles is low. Even with increased uncertainty in the fiber angles, i.e. higher σ_θ, there is no significant change in the optimal design.

4.5. Optimal frequency response of laminates subjected to static loads

If the laminate is subjected to significant static loads, static failure modes may become critical for many of the configurations generated during the optimization process. In such cases, search for optimal frequency response should be conducted within the feasible domain, in which the laminate configurations have sufficient strength to resist the applied loads. In order to achieve this, penalty functions are defined and added to the objective function value whenever a configuration within the infeasible domain is generated. The objective function for the maximum frequency separation then becomes

$$f = -(\Omega_{i+1}-\Omega_i)+w_1P-w_2\,\mathrm{SF} \tag{29}$$

where P is the penalty value, SF is the safety factor, w_i are suitable coefficients ($w_1=100$, $w_2=0.1$). SF is defined as the ratio of the stress causing failure to the stress induced by the expected loads as in engineering design practice. Values less than 1.0 indicate failure. The larger is the safety factor above 1.0, the safer is the laminate. In order to determine the failure load, Tsai–Wu criterion together with the maximum stress criterion is used. Stresses in the principal material directions are obtained by carrying out structural analysis using the classical lamination theory. In order to calculate the safety factor according to the maximum stress criterion the following procedure is used: the safety factor against the loading in the fiber direction is defined as $SF=X_t/\sigma_{11}$ if σ_{11} is tensile or $SF=X_c/\sigma_{11}$ if σ_{11} is compressive. Here X_t and X_c are the tensile and compressive strengths along the fiber direction, respectively. Similarly, safety factors against the transverse and shear loadings are also calculated. This procedure is repeated for each lamina and then the lowest safety factor is denoted as the safety factor of the laminate. If any one of the calculated safety factors is less than one, a penalty value is calculated as $P=(1/SF)-1$. The largest penalty value is chosen as the penalty value of the laminate. By a similar procedure safety factors and penalty values are calculated using Tsai–Wu criterion. The details regarding the calculation of SF and P are given in reference [30]. Because the coefficient, w_1, in front of P is large, whenever a configuration is generated in the infeasible domain, where static failure is predicted, objective function value is greatly increased. The magnitude of w_1 is selected such that even a small incursion into the infeasible domain will generate penalty values close to the frequency difference, $(\Omega_{i+1}-\Omega_i)$. This will lead the optimization away from the infeasible domain. SF of the configuration is subtracted from the objective function value to bias the stronger laminate designs. Because the coefficient, w_2, in front of SF is chosen to be small, this term becomes very small in comparison to the value of the frequency term; then the optimization will not be a multi-objective optimization in which both the strength and frequency difference are maximized. Instead, the search algorithm will prefer a stronger laminate design over a safe but weaker design having about the same frequency difference.

Numerical results were obtained for a graphite/epoxy material, T300/5308, using the aforementioned design optimization procedure and taking Eq. (29) as the objective function. Fiber orientation angles of a symmetric laminate having two distinct laminae, $[\alpha_4/\beta_4]_s$, were optimized. The thickness of each ply was 0.127 mm. a/b ratio was taken as 1.2. The material properties are given in reference [30]. Table 12 presents the results. If there is no static loading, the maximum frequency difference is obtained to be 372.666 with a layup of $[-8_4/86_4]_s$. When the plate is subjected to uniaxial in-plane load, N_{xx}, search for the maximum frequency difference is limited to safe designs in which SF is greater than 1.0 according to both static failure criteria. Because the load is uniaxial (only $N_{xx}\neq 0$), the strongest laminate design is $[0_8]_s$. If the load is small, the layup giving the largest frequency difference $[-8_4/86_4]_s$ is strong enough to resist the applied load; so the same optimal laminate design is obtained. If the load gets larger, static failure mode becomes critical and the fiber orientation angle should be chosen closer to the loading direction, which is 0°, to avoid static failure. When the load is increased to 1500 kN/m, the optimal laminate design is found to be $[-16_4/16_4]_s$, which yields the largest frequency difference and at

Table 12
Optimum lamina angles for maximum frequency separation for a laminate subjected to static loads. The lay-up configuration is $[\alpha_4/\beta_4]_S$.

Loading $N_{xx}/N_{yy}/N_{xy}/M_{xx}/M_{yy}/M_{xy}/$	Optimum design	Frequency difference, $\Delta\Omega_{12}$	Safety factor for Tsai–Wu	Safety factor for max. stress
0/0/0/0/0/0	$[-8_4/86_4]_s$	372.666	–	–
100/0/0/0/0/0	$[-5_4/86_4]_s$	372.508	1.006	1.009
500/0/0/0/0/0	$[-23_4/44_4]_s$	353.063	1.015	1.057
1000/0/0/0/0/0	$[-25_4/24_4]_s$	339.786	1.062	1.028
1500/0/0/0/0/0	$[-16_4/16_4]_s$	325.279	1.023	1.008
0/0/0/0/0/52	$[-3_4/83_4]_s$	371.498	1.005	1.006
0/0/0/0/0/55	$[-6_4/76_4]_s$	368.931	0.973	0.989
0/0/0/0/0/85	$[-6_4/76_4]_s$	368.931	0.629	0.640

the same time *SF* greater than 1.0. If the laminate is subjected to a twisting moment, M_{xy}, similarly the algorithm tries to get away from the infeasible region. If the load gets larger, the feasible domain becomes smaller; finally the entire solution domain becomes infeasible, i.e. SF is less than 1.0 for all possible designs. In that case, because w_1 in Eq. (29) is large, the penalty term dominates. The algorithm tries to maximize the strength without much sacrificing from the frequency response. Accordingly, for $M_{xy}=55$ Nm/m or $M_{xy}=85$ Nm/m, the algorithm yields the strongest laminate design as the optimal designs. Another alternative design, $[84_4/-14_4]_s$, having the same SF is eliminated because its frequency difference is small.

4.6. Comparative performances of SA algorithms

In order to see the relative performance of the SA algorithm proposed in the present study, a comparative study was conducted. Performance of a global search algorithm is defined as the number of times the global optimum is found divided by the number of functional evaluations. This is called reliability index, *Rel*.

$$Rel = \frac{\text{No of global optimums}}{\text{No of functional evaluation}} \tag{30}$$

This parameter reflects both reliability and efficiency of the algorithm. If its reliability is high, i.e. the probability of finding the global minimum is high, the numerator will be high. If its efficiency is high, i.e. the number of iterations required for convergence is low, the denominator will have a small value. Both of these will result in a higher value for the parameter.

Four different SA algorithms were considered: the present one, the classical simulated annealing algorithm (SA) [55], the direct search simulated annealing (DSA) [36], and the modified direct search simulated annealing (MDSA) proposed in a previous study [30]. SA algorithms are basically characterized by five features: Random generation of a new configuration, acceptance criterion for the newly generated configuration, the scheme used for the replacement of a current configuration with the accepted configuration, number of iterations executed at the current temperature, the scheme used for the reduction of the temperature parameter. In all SA variants, acceptability of a configuration is decided according to the probability of Boltzman distribution as given in Eq. (18). DSA differs from the classical SA mainly by its use of a set of current configurations like GA rather than a single current configuration. The main difference between DSA and MDSA is in the scheme used to generate random configurations. In MDSA, the neighborhood of the current point within which a new configuration is randomly chosen becomes narrower and narrower throughout the optimization process. This is achieved by decreasing $\Delta\theta_{\max}$ in Eq. (16) using Eq. (20), according to the procedure explained before. On the other hand, in DSA the maximum variation that can be introduced to the variables, $\Delta\theta_{\max}$, is not changed; it is taken as 5°. There are two basic differences between MDSA and the present method. Firstly, the replacement scheme is different. In MDSA, if a new configuration is accepted, it replaces the worst current configuration. In the present method, it replaces a current configuration randomly chosen among the worst $(n+1)$ configurations. Secondly, the cooling scheme is different. In the present method, the rate of reduction of the temperature parameter, $T_{\boldsymbol{k}}$, is made dependent on the reduction of $\Delta\theta_{\max}$ through Eq. (21). On the other hand, in MDSA, the values chosen for the upper and lower limits of α in Eq. (19), dictate the cooling rate.

Reliability indices are normalized by dividing their value by the reliability index of the present search algorithm, Rel_c, to obtain what is called performance index, *PI*.

$$PI = 100\frac{Rel}{Rel_c} \tag{31}$$

For the comparative study, the problem of thickness minimization of a laminate subjected to static loading was chosen instead of frequency response optimization. This was because the optimization process was repeated more than 300 times in order to calculate the value of the reliability index for each search algorithm and static analysis using the classical lamination theory took much shorter time than the frequency analysis using Chaudhuri's method. However, the conclusions drawn based on the results regarding the relative performances of the algorithms can be assumed to be valid for typical composite optimization problems, considering that innumerable local optimums were typically observed in different types of composite optimization problems in the previous studies.

A laminate subjected to pure twisting moment, $M_{xy}=10$ kNm/m, was considered in the comparative study. The interval between fiber orientation angles was chosen as 1°. The analysis was carried out using the method explained in reference [30] for a graphite/epoxy material, T300/5308, with the material properties given in that reference. Different numbers for distinct laminae were tried. Especially when this number was high, numerous near global optimum designs were obtained. For example, if the laminate consisted of 16 distinct laminae (32 design variables), the minimum thickness was obtained as 206 plies in 18% of the runs using the present method. The layup sequences of these laminate designs were all found to be different having safety factors ranging from 1.001 to 1.012. The best of these lay-ups was $[-80_{21}/-77_9/13_8/-74_3/15_6/-72_5/18_9/21_{10}/27_7/35_5/52_{11}/-37_8/55_1]_s$. In 80% of the runs, the minimum number of plies was 208; in 2% of the runs, it was 210. In calculating the reliability index, all of the near global optimums were taken as the global optimum considering that the safety factors were very close to each other, then the number of runs in which the minimum thickness was found to be 206 was divided by the total number of iterations to calculate the reliability index. Similarly, the reliability indices and then performance indices of the other algorithms were calculated. Table 13 presents the results. The performance index of the present method is 100 by definition. As expected the performance of the present method is better than MDSA especially for problems with a high number of optimization variables. The performances of DSA and SA are rather poor. This indicates the importance of reducing the search domain during the optimization process, which is the basic difference between MDSA and DSA. As Table 13 indicates, the relative performances of the SA algorithms depend on the number of optimization variables, i.e. the difficulty of the problem. If comparisons are conducted for a different type of optimization problem, the relative performances will also be different. However, the performance of the present algorithm is expected be superior for difficult combinatorial optimization problems.

4.7. Comparative performances of a genetic algorithm and the present SA algorithm

Lopez et al. [58] minimized the thickness of composite laminates subjected to static in-plane loads using a genetic algorithm. They compared the performances of their genetic algorithm and the one proposed by Le Riche and Haftka [59] using the performance criterion provided in that reference and found theirs better. In the performance criterion, a practical optimum is defined as the local optimum close to the global optimum by 0.1%. Then, the reliability of the algorithm is

Table 13
Comparison of the performances of various simulated annealing algorithms.

Number of distinct fiber angles	Minimum number of plies	Performance Index (*PI*)			
		Present SA	Modified DSA [30]	DSA [36]	SA [55]
16	206	100	62	0	0
8	208	100	85	1	0
4	212	100	98	33	15
2	218	100	105	50	22

Table 14
Comparison of the reliabilities of the genetic algorithm used by Lopez et al. [58] and the present algorithm. $N_{xx}=3000$ N/mm, $N_{yy}=3000$ N/mm.

N_{xy} (N/mm)	Optimum lay-up sequences	Failure criterion[a]	Safety factor	Reliability	
				Ref. [58]	Present
0	$[\pm 45_{17}]_s$, $[0_{10}/\pm 45_7/90_{10}]_s$…	MS	1.0455	1.00	1.00
0	The same	TW	1.1599	0.99	1.00
100	$[\pm 45_{17}]_s$	MS	1.0245	1.00	1.00
100	The same	TW	1.1412	1.00	1.00
250	$[0_{18}//90_{16}]_s$, $[0_{16}//90_{18}]_s$	MS	1.0117	0.77	0.84
250	The same	TW	1.0161	0.32	0.59
500	$[\pm 45_{18}]_s$	MS	1.0041	0.96	1.00
500	The same	TW	1.1243	1.00	1.00
1000	$[\pm 45_{20}]_s$	MS	1.0209	0.96	1.00
1000	The same	TW	1.1302	0.41	1.00

[a] MS and TW denote the maximum stress criterion and Tsai–Wu criterion, respectively.

defined as the probability that the algorithm finds a practical optimum in 6000 functional evaluations. This probability is calculated after conducting hundreds of independent runs; then the number of times that a practical optimum is found is divided by the number of runs. Table 14 presents the optimum lay-up sequences of laminates subjected to various in-plane loads and the reliabilities of the genetic algorithm used by Lopez et al. [58] and the present algorithm. The laminate design is $[0_{2q}/\pm 45_r/90_{2u}]_s$, where q, r, and u are the integer variables used to minimize the thickness. This means that there are only three optimization variables. In order for the optimization process to converge in 6000 iterations, the value of factor c in Eq. (20) was chosen as 0.82 and the initial values of the maximum variation for thickness [30], $\Delta n_{\max}$, and angle were chosen as 12 and 90°, respectively. As seen in the table, the reliability of the present algorithm is better for this problem whether Tsai–Wu or the maximum stress is used as the failure criterion; but the real difference is expected to manifest itself for problems with high numbers of optimization variables.

5. Conclusions

In this study, frequency response of symmetric laminated plates was optimized. In order to calculate natural frequency, an analytic method accounting for the effects of bending–twisting coupling was used. For this reason, there was no need to impose limitations on the values of fiber orientation angles or on the stacking sequence. Otherwise, imposing restrictions on stacking sequence or the possible fiber orientations would result in worse optimum designs. Because of the existence of numerous local optimums, a reliable global search algorithm, a variant of simulated annealing, was used. Discrete fiber angles were taken as design variables. Firstly, a convergence analysis was carried out in order to determine the number of Fourier series terms sufficient to obtain an acceptable accuracy, because the accuracy of the calculated values of frequency was observed to have a significant effect on the optimization results. After ensuring accurate prediction of the mechanical behavior of the laminate, comparisons were made between the results obtained using the present optimization procedure and the results obtained in previous studies for the fundamental frequency maximization and adjacent frequency separation problems. Some discrepancies were observed in the results, which may only be attributed to the negligence of bending–twisting coupling in those studies. Therefore, negligence of this effect cannot be justified in general design optimization studies. However, the results were in agreement for the studies that used approximate methods like FEM accounting for this coupling.

The optimum results were obtained for rectangular graphite/epoxy laminates having different aspect ratios with simply-supported edges using different design domains. By increasing the number of distinct lamina angles and the range of values they may take, one may obtain a larger design domain, i.e. more lay-up configurations become possible. In this study, up to sixteen distinct fiber angles with 1° angle increments were used as design variables to optimize laminates. To the knowledge of the authors, optimization with such a large solution domain was not attempted in the previous studies. With a larger domain, it was possible to obtain a better optimum design. Optimization process was repeated for different aspect ratios in order to determine the effect of geometry on the optimum frequency. The optimum configurations were observed to strongly depend on the plate aspect ratio.

Fundamental frequency maximization problems in which fiber angles were treated as random variables were also considered. Optimum designs obtained with random angles were different from the ones in which angles showed no variation. However the difference was found to be small even for cases in which the degree of uncertainty was high.

Frequency response optimization subjected to static failure constraints was also performed. Tsai–Wu and the maximum stress criteria were jointly used to determine the failure behavior of laminates under static loads. Search for the optimum frequency response thus was restricted to feasible domain in which the laminate configuration had sufficient strength against the applied loading.

The search algorithm proposed in this study has basically two advantages over the previous versions of the SA algorithm. Firstly, it is computationally more efficient, especially when the number of optimization variables is high, as the comparative study shows. Secondly, the present algorithm is better regarding the ease of application. Its convergence is made dependent on only a single parameter (the factor, c, in Eq. (20)). On the other hand, suitable values should be found for a number of parameters for the effective use of the other algorithms.

If the complexity of the geometry does not allow use of an analytical method, the structural analysis can be carried out using FE method. In that case, the same search algorithm can be used to find the optimum lamina angles. However, for a large structure having complex geometry, the computational time may become so long that use of a stochastic search algorithm may become impracticable in a design process. In that case, a more efficient search algorithm should be used. The best candidate may be a hybrid algorithm, in which a local search algorithm is used to find the optimal lamination parameters at the first level and then a global search algorithm like the one proposed in this study is used to find the optimal lamina angles corresponding to the optimal lamination parameters at the second level.

Acknowledgment

This paper is based on the work supported by TUBITAK (The Scientific and Technological Research Council of Turkiye) with the code number 106M301.

References

[1] C.W. Bert, Optimal design of a composite-material plate to maximize its fundamental frequency, *Journal of Sound and Vibration* 50 (1977) 229–237.

[2] C.W. Bert, Design of clamped composite-material plates to maximize fundamental frequency, *Journal of Mechanical Design* 100 (1978) 274–278.

[3] R. Reiss, S. Ramachandran, Maximum frequency design of symmetric angle-ply laminates, in: I.H. Marshall (Ed.), *Composite Structures 4, Vol. 1: Analysis and Design Studies*, Elsevier, London, 1987, pp. 1476–1487.

[4] H.C. Mateus, C.M.M. Soares, C.A.M. Soares, Sensitivity analysis and optimal design of thin laminated composite structures, *Computers & Structures* 41 (1991) 501–508.

[5] C.M.M. Soares, V.F. Correia, H. Mateus, A discrete model for the optimal design of thin composite plate-shell type structures using a two-level approach, *Composite Structures* 30 (1995) 147–157.

[6] S.S. Rao, K. Singh, Optimum design of laminates with natural frequency constraints, *Journal of Sound and Vibration* 67 (1979) 101–112.

[7] V.M.F. Correia, C.M.M. Soares, C.A.M. Soares, Higher order models on the eigenfrequency analysis and optimal design of laminated composite structures, *Composite Structures* 39 (1997) 237–253.

[8] Y. Narita, Layerwise optimization for the maximum fundamental frequency of laminated composite plates, *Journal of Sound and Vibration* 263 (2003) 1005–1016.

[9] Y. Narita, J.M. Hodgkinson, Layerwise optimisation for maximising the fundamental frequencies of point-supported rectangular laminated composite plates, *Composite Structures* 69 (2005) 127–135.

[10] Y. Narita, P. Robinson, Maximizing the fundamental frequency of laminated cylindrical panels using layerwise optimization, *International Journal of Mechanical Sciences* 48 (2006) 1516–1524.

[11] Y. Narita, X. Zhao, An optimal design for the maximum fundamental frequency of laminated shallow shells, *International Journal of Solids and Structures* 35 (1998) 2571–2583.

[12] A.W. Blom, S. Setoodeh, J.M.A.M. Hol, Design of variable-stiffness conical shells for maximum fundamental eigenfrequency, *Computers & Structures* 86 (2008) 870–878.

[13] M.M. Abdalla, S. Setoodeh, Z. Gürdal, Design of variable stiffness composite panels for maximum fundamental frequency using lamination parameters, *Composite Structures* 81 (2007) 283–291.

[14] H.T. Hu, J.Y. Tsai, Maximization of the fundamental frequencies of laminated cylindrical shells with respect to fiber orientations, *Journal of Sound and Vibration* 225 (1999) 723–740.

[15] C.G. Diaconu, M. Sato, H. Sekine, Layup optimization of symmetrically laminated thick plates for fundamental frequencies using lamination parameters, *Structural and Multidisciplinary Optimization* 24 (2002) 302–311.

[16] M.K. Apalak, M. Yildirim, R. Ekici, Layer optimisation for maximum fundamental frequency of laminated composite plates for different edge conditions, *Composites Science and Technology* 68 (2008) 537–550.

[17] M. Abachizadeh, M. Tahani, An ant colony optimisation approach to multi- objective optimal design of symmetric hybrid laminates for maximum fundamental frequency and minimum cost, *Structural and Multidisciplinary Optimization* 37 (2009) 367–376.

[18] N.L. Pedersen, On simultaneous shape and orientational design for eigenfrequency optimization, *Structural and Multidisciplinary Optimization* 33 (2007) 387–399.

[19] N.L. Pedersen, On design of fiber-nets and orientation for eigenfrequency optimization of plates, *Computational Mechanics* 39 (2006) 1–13.

[20] N.L. Pedersen, Eigenfrequency optimization of fiber reinforced plates using optimality criteria and mathematical programming, *6th World Congresses of Structural and Multidisciplinary Optimization*, Rio de Janeiro, Brazil, June 2005.

[21] S. Adali, V.E. Verijenko, Optimum stacking sequence design of symmetric hybrid laminates undergoing free vibrations, *Composite Structures* 54 (2001) 131–138.

[22] B. Farshi, R. Rabiei, Optimum design of composite laminates for frequency constraints, *Composite Structures* 81 (2007) 587–597.

[23] K.J. Duffy, S. Adali, Optimal fibre orientation of antisymmetric hybrid laminates for maximum fundamental frequency and frequency separation, *Journal of Sound and Vibration* 146 (1991) 181–190.

[24] C.M.M. Soares, C.A.M. Soares, H.C. Mateus, A model for the optimum design of thin laminated plate-shell structures for static, dynamic and buckling behaviour, *Composite Structures* 32 (1995) 69–79.

[25] Y. Narita, G.J. Turvey, Maximizing the buckling loads of symmetrically laminated composite rectangular plates using a layerwise optimization approach, *Proceedings of the Institution of Mechanical Engineers, Part C* 218 (2004) 681–691.

[26] O. Seresta, S.B. Mulani, M.M. Abdalla, Stacking sequence design of laminated composite plates for maximum flutter velocity and buckling capacity with stability constraint. *46th AIAA/ASME/ASCE/AHS/ASC Structures, Structural Dynamics & Materials Conference*, Austen, Texas, April 2005.

[27] K. Sivakumar, N.G.R. Iyengar, K. Deb, Optimum design of laminated plates with cutouts using a genetic algorithm, *Composite Structures* 42 (1998) 265–279.

[28] D.B. Adams, L.T. Watson, Z. Gürdal, Genetic algorithm optimization and blending of composite laminates by locally reducing laminate thickness, *Advances in Engineering Software* 35 (2004) 35–43.

[29] O. Erdal, F.O. Sönmez, Optimum design of laminates for maximum buckling load capacity using simulated annealing, *Composite Structures* 71 (2005) 45–52.

[30] M. Akbulut, F.O. Sönmez, Optimum design of composite laminates for minimum thickness, *Computers & Structures* 86 (2008) 1974–1982.

[31] J.M.S. Moita, V.M.F. Correia, P.G. Martins, Optimal design in vibration control of adaptive structures using a simulated annealing algorithm, *Composite Structures* 75 (2006) 79–87.

[32] J. Chen, R. Ge, J. Wei, Probabilistic optimal design of laminates using improved particle swarm optimization, *Engineering Optimization* 40 (2008) 695–708.

[33] F.T. Lin, C.Y. Kao, C.C. Hsu, Applying the genetic approach to simulated annealing in solving some NP-hard problems, *IEEE Transactions on Systems, Man and Cybernetics* 23 (1993) 1752–1767.

[34] H. Chen, N.S. Flann, D.W. Watson, Parallel genetic simulated annealing: a massively parallel SIMD algorithm, *IEEE Transactions on Parallel and Distributed Systems* 9 (1998) 126–136.

[35] W.C. Jackson, J.N. Norgard, A hybrid genetic algorithm with boltzmann convergence properties, *Journal of Optimization Theory and Applications* 136 (2008) 431–443.

[36] M.M. Ali, A. Törn, S. Viitanen, A direct search variant of the simulated annealing algorithm for optimization involving continuous variables, *Computers & Operations Research* 29 (2002) 87–102.

[37] J. Kennedy, R. Eberhart, Particle swarm optimization, *Proceedings of IEEE International Conference on Neural Networks* 4 (1995) 1942–1948.

[38] S.S. Mahapatra, S. Biswas, Permutation flow shop scheduling using particle swarm optimisation with mutation, *IE(I) Journal-MC* 89 (2008) 24–28.

[39] Z.B. Lu, A. Zhang, X.Y. Hou, Pattern synthesis of cylindrical conformal array by the modified particle swarm optimization algorithm, *Progress in Electromagnetics Research* 79 (2008) 415–426.

[40] L. Fang, P. Chen, S. Liu, Particle swarm optimization with simulated annealing for TSP. Proc. of the 6th Conference on 6th WSEAS International Conference on Artificial Intelligence, Knowledge Engineering and Data Bases 6, Corfu Island, Greece, February 2007, pp. 206–210.

[41] B. Baumann, B. Kost, Structure assembling by stochastic topology optimization, *Computers & Structures* 83 (2005) 2175–2184.

[42] J.E. Herencia, P.M. Weaver, M.I. Friswell, Initial sizing optimization of anisotropic composite panels with T-shaped stiffeners, *Thin-Walled Structures* 46 (2008) 399–412.

[43] A. Todoroki, R.T. Haftka, Stacking sequence optimization by a genetic algorithm with a new recessive gene like repair strategy, *Composites Part B* 29B (1998) 277–285.

[44] A. Todoroki, M. Sasai, Stacking sequence optimizations using GA with zoomed response surface on lamination parameters, *Advanced Composite Materials* 11 (2003) 299–318.
[45] A. Todoroki, T. Ishikawa, Design of experiments for stacking sequence optimizations with genetic algorithm using response surface approximations, *Composite Structures* 64 (2004) 349–357.
[46] M. Sekishiro, A. Todoroki, Extended fractal branch and bound method for optimization of multiple stacking sequences of stiffened composite panel, *Advanced Composite Materials* 15 (2006) 341–356.
[47] A. Todoroki, Y. Terada, Improved fractal branch and bound method for stacking-sequence optimizations of laminates, *American Institute of Aeronautics and Astronautics Journal* 42 (2004) 141–148.
[48] A. Todoroki, R.T. Haftka, Stacking sequence matching by two-stage genetic algorithm with consanguineous initial population, *American Institute of Aeronautics and Astronautics Journal* 97–1228 (1997) 1297–1302.
[49] R.A. Chaudhuri, On the roles of complementary and admissible boundary constraints in fourier solutions to the boundary value problems of completely coupled *r*th order PDEs, *Journal of Sound and Vibration* 251 (2002) 261–313.
[50] R.A. Chaudhuri, K. Balaraman, V.X. Kunukkasseril, A combined theoretical and experimental investigation on free vibration of thin symmetrically laminated anisotropic plates, *Composite Structures* 67 (2005) 85–97.
[51] M.P. Nemeth, Importance of anisotropy on buckling of compression-loaded symmetric composite plates, *American Institute of Aeronautics and Astronautics Journal* 24 (1986) 1831–1835.
[52] R.M. Jones, *Mechanics of Composite Materials*, 2nd ed., Taylor & Francis, Philadelphia, 1999.
[53] P. Cupial, Calculation of the natural frequencies of composite plates by the Rayleigh–Ritz method with orthogonal polynomials, *Journal of Sound and Vibration* 201 (1997) 385–387.
[54] A.W. Leissa, Y. Narita, Vibration studies for simply supported symmetrically laminated rectangular plates, *Composite Structures* 12 (1989) 113–132.
[55] S. Kirkpatrick, C.D. Gelatt, M.P. Vecchi, Optimization by Simulated Annealing, *Science* 220 (1983) 671–680.
[56] F.X. Irisarri, D.H. Bassir, N. Carrere, J.F. Maire, Multiobjective stacking sequence optimization for laminated composite structures, *Composites Science and Technology* 69 (2009) 983–990.
[57] A. Haldar, S. Mahadevan, *Probability, Reliability, and Statistical Methods in Engineering Design*, John Wiley & Sons, New York, 2000.
[58] R.H. Lopez, M.A. Luersen, E.S. Cursi, Optimization of laminated composites considering different failure criteria, *Composites: Part B* 40 (2009) 731–740.
[59] R. Le Riche, R. Haftka, Improved genetic algorithm for minimum thickness composite laminate design, *Composites Engineering* 5 (1995) 143–161.